TOPOLOGICAL STUDY OF TORSIONAL SPINE MAGNETIC RECONNECTION AT NULL POINT

*** Ali Khalaf Hussain Al-hachami** ****Ali Husein Shuaa Al-taie**
***Wassit university/college of science Physics department ** Wassit university/college of science Biology department**

الخلاصة

العمود الفقري هو خط المجال المعزول الذي يقترب من النقطة الملغية (أو يتراجع عنها)، ما يسمى أعادة الربط المغناطيسي في العمود الفقري الملتوي الذي يحدث عند خطوط حقل المجال المغناطيسي في المنطقة المجاورة للمروحة، وأن التيار يتركز على طول العمود الفقري بحيث أن خطوط الحقل المغناطيسي المجاور يخضع إلى انزلاق التناوب. في هذا النظام العمود الفقري والمروحة يكونان متعامدين وليس هناك نقل في التدفق عبر العمود الفقري أو المروحة . هندسة طبقة التيار ضمن إعادة الربط في العمود الفقري الملتوي الذي يحدث تعتمد بشدة على التماثل للحقل المغناطيسي. أعادة ربط العمود الفقري الملتوي يحدث في أنبوب ضيق حول العمود الفقري، مع مقطع عرضي بيضاوي الشكل عندما القيم الذاتية تكون مختلفة .والانحراف في القطع الناقص يزداد عند زيادة درجة عدم التماثل ، ضمن المحور القصير للقطع الناقص يجري على طول اتجاه المجال القوي . أيضا تم العثور على الذروة للتيار، ومعدل إعادة الاتصال القياسية ، لا تعتمد بشدة على درجة التماثل.

ABSTRACT

The spine is an isolated field line which approaches the null (or recedes from it), so called *torsional spine reconnection* occurs when field lines in the vicinity of the fan rotate, with current becoming concentrated along the spine so that nearby field lines undergo rotational slippage. In of these region, the spine and fan are perpendicular and there is no flux transfer across spine or fan. The geometry of the current layers within which torsional spine reconnection occur is strongly dependent on the symmetry of the magnetic field. Torsional spine reconnection occurs in a narrow tube around the spine, with elliptical crosssection when the fan eigenvalues are different. The eccentricity of the ellipse increases as the degree of asymmetry increases, with the short axis of the ellipse being along the strong field direction. The spatiotemporal peak current, and the peak reconnection rate attained, are found not to depend strongly on the degree of asymmetry.

1- INTRODUCTION

Magnetic reconnection is a fundamental process in many areas of plasma physics, whereby the magnetic field, **B**, becomes restructured. When null points are present the global topology of the field changes. Our ideas on how this restructuring occurs come mostly from the well-studied case of reconnection in two dimensions. In two dimensions, reconnection occurs at hyperbolic null points of the magnetic field (see, e.g. Priest and Forbes, 2000 [1], for a review), commonly known as X-points (see Figure 1). A plasma flow transports magnetic flux towards the X-point, where the reconnection takes place, and the flow then transports the reconnected magnetic flux away from the X-point. In terms of magnetic field lines, the process of reconnection involves a pair of field lines being brought in from two quadrants on opposite sides of the null. At the X-point each of these field lines breaks, when they lie along the separatrices of the field. They are then rejoined and move out in the other two quadrants of **B**. The result is that the field line footpoints are pair-wise differently connected when they leave the reconnection region. Magnetic reconnection is a fundamentally non-ideal process; in an ideal plasma, magnetic field lines maintain their identity for all time, and are said to be ‘frozeninto’ the plasma. The non-idealness may be the result, for example, of a non-zero resistivity, ή, in which case, assuming no other non-ideal effects are important, the process satisfies Ohm’s law in the form [7]

$$\mathbf{E} + \mathbf{v}\times \mathbf{B} = \acute{\eta}\mathbf{J},$$

Where **E, v, B,** ή and **J** are the electric field, velocity, magnetic field, resistivity and electric current respectively.

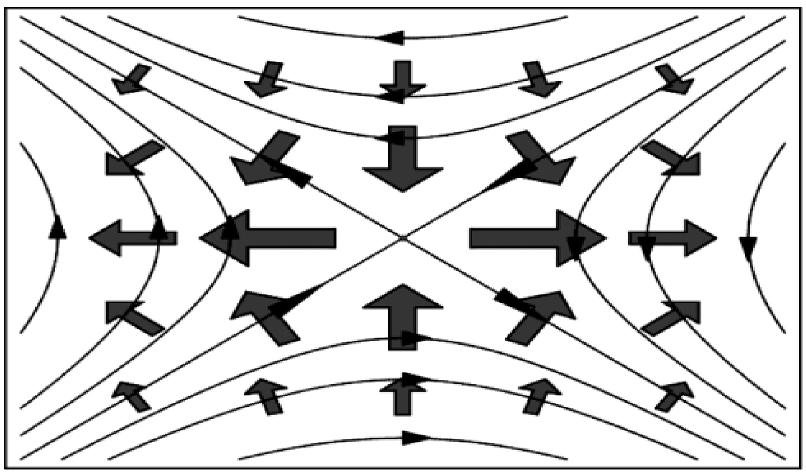

FIGURE 1 Two-dimensional reconnection at an X-point. The thin lines are magnetic field lines and the bold arrows indicate the direction of the plasma flow.

2- STRUCTURE OF THREE DIMENSION NULL POINTS

The simplest linear null point (for which the magnetic field increases linearly from the null) has field components

$$\boldsymbol{B} = \frac{B_0}{L_0}(x, y, -2z),\ L_0 \neq 0 \qquad (1)$$

in Cartesian coordinates or

$$\boldsymbol{B} = \frac{B_0}{L_0}(r, 0, -2z),\ L_0 \neq 0$$

in cylindrical polar so that $\nabla \cdot \mathbf{B} = 0$ identically, where B_0 and L_0 are constant. The field lines are given by

$$y = mx, \qquad z = \frac{n}{x^2}, \qquad x \neq 0$$

where m and n are constants. The z-axis is the spine and the xy-plane is the fan. For this so-called proper radial null the fan field lines are straight [Figure 2a]. It is a particular member (with a=1) of a wider class of current-free improper radial null points $a \neq 1$with curved fan field lines, having field components

$$\boldsymbol{B} = \frac{B_0}{L_0}[x, ay, -(a+1)z], \qquad L_0 \neq 0$$

This is the generic form for a current-free null since the proper radial null is structurally unstable in the sense that it occurs only for a particular value of a, but for simplicity much of the theory so far has used a proper radial null. More generally, each of the three field components of a linear null may be written in terms of three constants, making nine in all. However, Parnell et al. [2] built on earlier work [3]–[4] and showed, by using $\nabla \cdot \mathbf{B}$ =0, by normalizing and by rotating the axes, that the nine constants may be reduced to four $(a, b, j_{||}, j_{\perp})$such that

$$\begin{pmatrix} B_x \\ B_y \\ B_z \end{pmatrix} = \frac{B_0}{L_0}\begin{pmatrix} 1 & \frac{1}{2}(b - j_{||}) & 0 \\ \frac{1}{2}(b + j_{||}) & -a & 0 \\ 0 & j_{\perp} & -(a+1) \end{pmatrix}\begin{pmatrix} x \\ y \\ z \end{pmatrix},$$

where $j_{||}$ is the current parallel to the spine and $j_{\perp}$ is the current perpendicular to the spine. Furthermore, both nulls and separators are susceptible to collapse to form current sheets when the boundary conditions allow it.

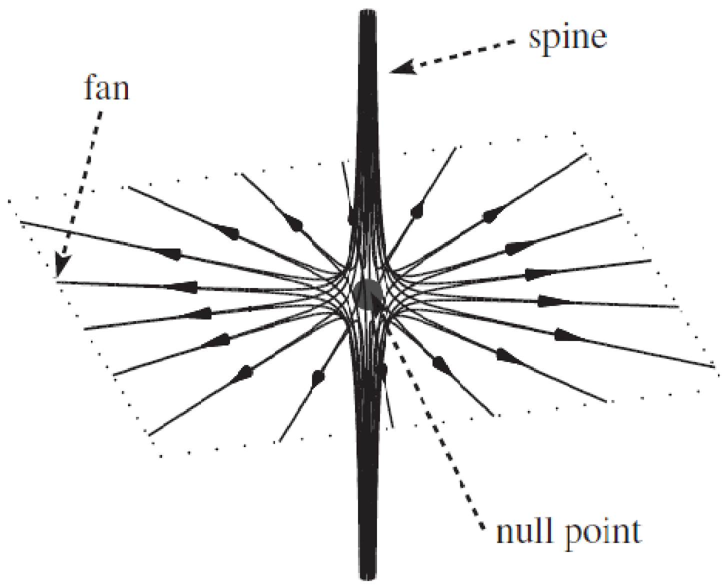

FIGURE 2. Field lines for a proper radial null.

3- General method

We seek to find solutions to the kinematic, steady state, resistive Magnetohydro- dynamic equations in the vicinity of a 3D magnetic null point. Thus, we solve

$$\mathbf{E} + \mathbf{v}\times \mathbf{B} = \acute{\eta}\mathbf{J}, \qquad (2)$$
$$\nabla\times \mathbf{E} = 0, \qquad (3)$$
$$\nabla\times \mathbf{B} = \acute{\eta}\mathbf{J}, \qquad (4)$$
$$\nabla \cdot \mathbf{B} = 0. \qquad (5)$$

From Eq. 3 we can express the electric field as $E=-\nabla\Phi$ where Φ is a scalar potential. The component of Equation (2) parallel to B

$$\mathrm{E} + \mathrm{v} \times \mathrm{B} = \acute{\eta}\mathrm{J}$$
$$\rightarrow \ \mathrm{E}.\mathrm{B} + (\mathrm{v} \times \mathrm{B}).\mathrm{B} = \acute{\eta}\mathrm{J}.\mathrm{B}$$
$$\rightarrow \ -\nabla\Phi.\mathrm{B} = \acute{\eta}\mathrm{J}.\mathrm{B}$$

Now, since $\frac{d\Phi}{ds} = \frac{d\Phi}{dx}.\frac{dx}{ds}$ by the chain rule and $\frac{d\Phi}{ds} = \mathrm{B}$, we have

$$\frac{d\Phi}{ds} = \nabla\Phi.\mathrm{B}$$
$$\frac{d\Phi}{ds} = -\acute{\eta}\mathrm{J}.\mathrm{B}$$

and we can calculate Φ by integrating along magnetic field lines:

$$\Phi = -\int \acute{\eta}\,\mathbf{J}\cdot\mathbf{B}\,ds + \Phi_0. \qquad (6)$$

where Φ_0 is a constant of integration. This integral is solved by using the field line equations in (x, y, z) expressed in terms of the parameter s and some initial position(x_0, y_0, z_0). The field line equations are obtained by solving

$$\frac{\partial X(s)}{\partial s} = \mathbf{B}(X(s)) \qquad (7).$$

These equations are invertible so φ can be represented as a function of s and initial position to carry out the integral in Eq. 6 and then transferred back into a function of x, y and z to find the electric field from

$$\mathbf{E} = -\nabla\Phi. \qquad (8)$$

Thus for a given magnetic configuration we can find the electric field due to nonideal effects (i.e., those due to $\mathbf{J} \neq 0$). Using this we can also find the resulting flow velocity perpendicular to the magnetic field by taking the vector product of Equation 2 with B to give

$$\mathbf{v}_{\perp} = \frac{E \; - J}{B} \qquad (9)$$

4- TORSIONAL SPINE RECONNECTION

The type of reconnection set up at 3D null depends crucially on the nature of the flows and boundary conditions that are responsible for the reconnection. Let us suppose first that a rotation of the fan plane drives a current along the spine and gives rise to torsional spine reconnection, as sketched in Figure 3a. The nature of the reconnection is that in the core of the spine current tube there is rotational slippage, with the field lines becoming disconnected and rotating around the spine (see Ref. 5): Figure 3b shows on the left side a particular magnetic field line and its plasma elements at $t = t_0$; in the upper part of the figure (above the shaded diffusion region) this field line and its attached plasma elements rotate about the spine through positions at times t_1, t_2, and t_3; in the lower part of the figure (below the diffusion region) the plasma elements that were on the field line at t_0 rotate to positions at t_1, t_2, and t_3 that are on different field lines. A steady kinematic solution may be found following the approach of Section 3. The electric field may be written as the sum ($\mathbf{E} = \nabla\Phi = \nabla\Phi_{nid} + \nabla\Phi_{id}$) of a nonideal pure (elementary) solution satisfying

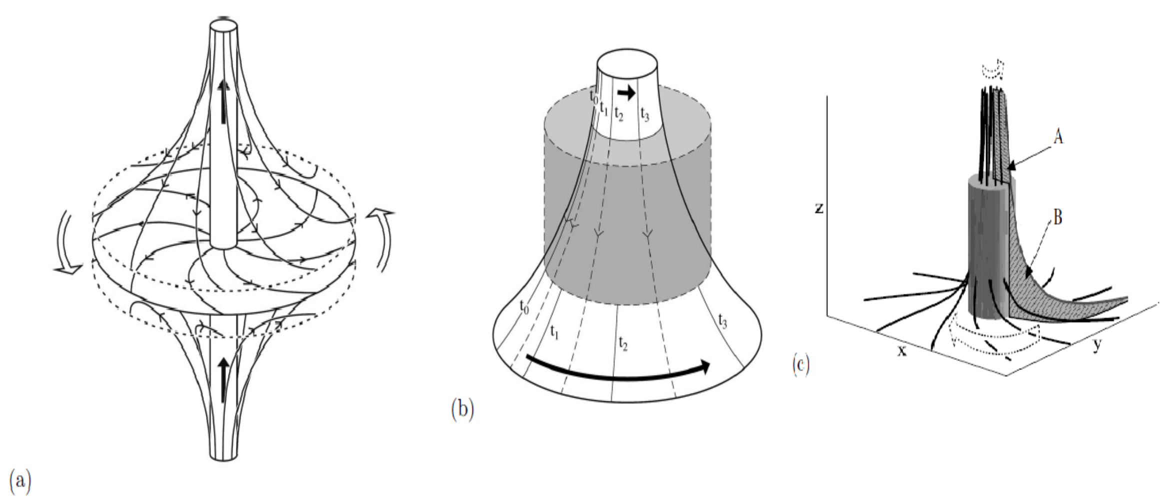

FIGURE 3. (a) A rotational motion of the fan (open arrows) driving torsional spine reconnection with a strong current (solid arrows) along the spine.(b) Rotational slippage of fields entering through the top of the diffusion region on a curved flux surface, showing as solid curves the locations of the plasma elements at $t = t_1$, $t = t_2$, and $t = t_3$, that initially ($t = t_0$) lay on one field line. (c) The reconnection rate measures a rotational mismatching of flux threading the diffusion region, namely, the difference between the rates of flux transport through surfaces A and B.

$$\boldsymbol{\nabla}\Phi_{nid} + \mathbf{v}_{nid} \times \boldsymbol{B} = \acute{\eta}\boldsymbol{\nabla} \times \mathbf{B},$$

and an ideal solution satisfying

$$\boldsymbol{\nabla}\Phi_{id} + \mathbf{v}_{id} \times \boldsymbol{B} = 0.$$

Consider a spiral magnetic null point

$$\boldsymbol{B} = \frac{B_0}{L_0}\left(R, \frac{1}{2}Rj, -2z\right), \quad L_0 \neq 0 \qquad (10)$$

and suppose the diffusion region is a cylinder of radius a and height $2b$ and that the magnetic diffusivity has the form $\acute{\eta} = \acute{\eta}_0(R, z)$, where $f(0,0) = 1$ and $f(R, z)$ vanishes on the boundary of the diffusion region and outside it. The field lines for this spiral null may be obtained by solving

$$\frac{dR}{ds} = \frac{L_0 B_R}{B_0} = R, \quad \frac{d\varphi}{ds} = \frac{L_0 B_\theta}{B_0} = \frac{1}{2}jR, \quad \frac{dz}{ds} = \frac{L_0 B_z}{B_0} = -2z, \quad B_0 \neq 0$$

Suppose we start a field line at the point $(R, \varphi, z) = (R_0, \varphi_0, z_0)$ at $s = 0$. Then the field line equations are

$$R = R_0 e^s, \quad z = z_0 e^{-2z}, \; \varphi = \varphi_0 + \tfrac{1}{2}js. \qquad (11)$$

These give a mapping from an initial point (R_0, φ_0, b) to any other point (R, φ, z)along a field line. The inverse mapping is

$$R_0 = Re^{-s}, \quad z_0 = ze^{2z}, \; \varphi_0 = \varphi - \tfrac{1}{2}js, \qquad (12)$$

where $s = -\frac{1}{2}\log(\frac{z}{z_0})$.

4.1 Pure solution

The pure elementary solution describes the core of the reconnection process. It is obtained following Refs. [5] and [10] by solving Equation (2), with Equations (3, (4), and 5. Thus we write $\mathbf{E} = -\nabla\,\Phi$. with Φ_{nid} (nonideal) given by Eq. (6) and set $\Phi_0 = 0$ so that the flow vanishes outside the diffusion region. Inside the diffusion region the flow and flux velocities have no component across either the spine or the fan. For the spiral magnetic field $(B_{\boldsymbol{R}}, B_{\boldsymbol{\varphi}}, B_{\boldsymbol{z}}) = \frac{B_0}{L_0}\left(R, \frac{1}{2}Rj, -2z\right)$ and mapping (11), Φ_{nid}becomes$\Phi_{nid} = -\Phi_{nid0} \int \frac{ή}{ή_0} e^{-2s} ds$, where $\Phi_{nid0} = \frac{2B_0 ή_0 b j_0}{\mu L_0}$. (μ is the magnetic permeability in vacuum). Then, once a form for ή is assumed, this may be integrated to give$\Phi_{nid}(s, R_0, \varphi_0)$. After using the inverse mapping (12), we can then deduce $\Phi_{nid}(R, \varphi, z)$ and therefore **E** and $\mathbf{v}_\perp$ everywhere. If a diffusion region is isolated, a change in connectivity of field lines may be studied, by following field lines anchored in the ideal region on either side of the diffusion region. A diffusion region is, in general, isolated if (ή**J)** is localized in space. In practical cases in astrophysics, this is likely to be mainly because **J** is localized but, in addition, sometimes because as a consequence ή is also localized. Some numerical simulations have a localized ή, whereas others have a uniform ή or a purely numerical dissipation. However the important feature in all these cases is that the product ή**J** is localized. Now, in each of our solutions below, we follow Refs. 6, 7, and 8 in choosing a spatially localized ή**J** by imposing a spatially localized resistivity profile together with a **J** that is not localized. The reason for doing this is to render the mathematical equations tractable since we have not yet discovered a way to do so with a localized **J**. The quantitative spatial profiles of physical quantities will depend on the ή profile, but the qualitative topological properties of the field line behavior in such models are expected to be generic and independent of the particular profile chosen for $ή$. There are four regions with different forms for Φ_{nid}, as illustrated in Figure 4, which shows a vertical cut in the first quadrant of the Rz-plane. In region (1) threaded by field lines that enter the diffusion region (shaded) from above, we assume $\Phi_{nid}(R, z) = 0$ so that there is no electric field or flow. The same is true in region (2) which lies above the flux surface $zR^2 = ba^2$ that touches the upper corner (a, b) of the diffusion region. We calculate below the forms of $\Phi_{nid}(R, z)$ in the diffusion region (3) and in region (4) threaded by field lines that leave the diffusion region through its sides. For example, let us assume that ή vanishes outside the diffusion region (D) and that inside D it has the form

$$ή = ή_0 \begin{cases} \left[1 - \left(\frac{R}{a}\right)^2\right]^2 \left[1 - \left(\frac{z}{b}\right)^2\right]^2, & R < a,\ z^2 < b^2 \\ 0 & otherwise \end{cases}$$

which peaks at the origin and vanishes on the boundary of D. First, we use mapping (11) to substitute for R and z, and integrate with respect to s from the point $T(R, b)$ on the top of D to the point $P(R, z)$ inside D (Figure 4). Then we use the inverse mapping (12) to replace $R_0$and s, and finally we obtain the potential throughout D (region 3) in Figure (4) as

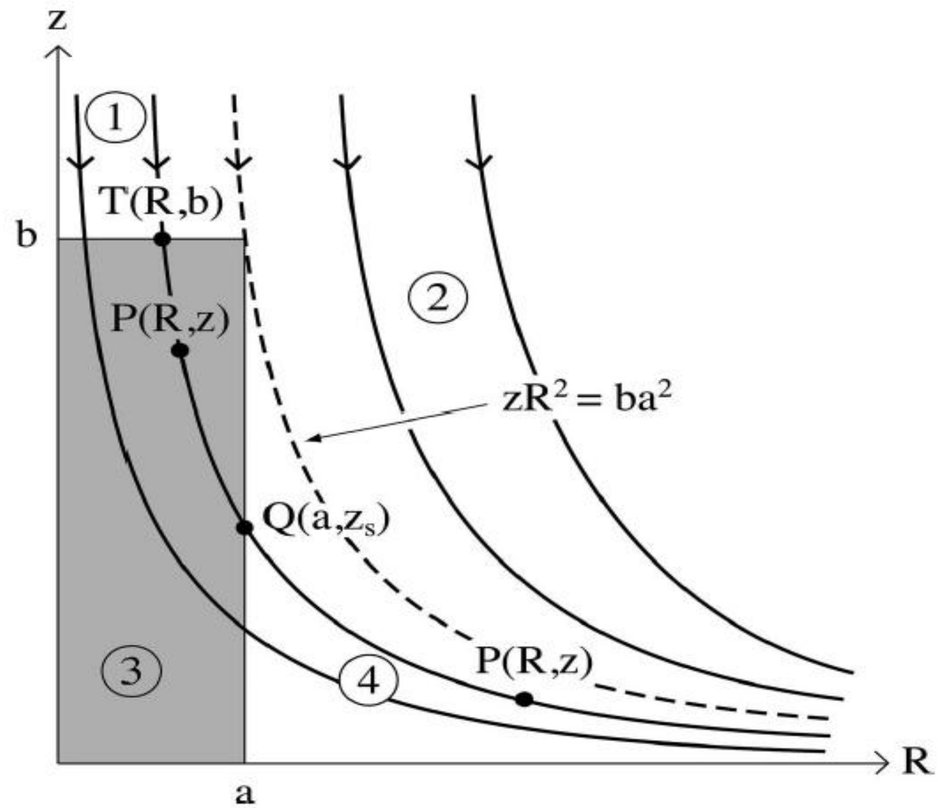

FIGURE 4. The projection of magnetic field lines and the diffusion region in the first quadrant of the rz-plane, showing four different regions, in which $\Phi_{nid}(R,z)$ is calculated. A magnetic field line whose projection intersects the top of the diffusion region in $T(R,b)$ and the side in $Q(\mathrm{a},z_s)$ contains typical points $P(R,z)$ inside and beyond the diffusion region. The bounding field line $zR^2 = ba^2$ is shown as dashed.

$$\Phi_{nid}(R,z) = -\frac{1}{2}\Phi_{nid0}\left[\left(1-\frac{z}{b}\right)-\frac{R^4}{a^4}\left(\frac{z}{b}-\frac{z^2}{b^2}\right)+\frac{1}{3}\left(\frac{z^3}{b^3}-1\right)+\frac{R^4}{a^4}\left(\frac{z^2}{b^2}-\frac{z^3}{b^3}\right)\right],\quad a \neq 0 \;\&\; b \neq 0. \qquad 13$$

This then determines the components of the electric field ($\mathbf{E} = \boldsymbol{\nabla}\Phi_{nid}$) everywhere in D as

$$\mathrm{E}_R = \frac{\partial \Phi_{nid}}{\partial R} = \frac{2\Phi_{nid0}R^3}{a^4}\left(\frac{z}{b}-\frac{2z^2}{b^2}+\frac{z^3}{b^3}\right), \qquad a \neq 0 \;\&\; b \neq 0$$

$$\mathrm{E}_z = \frac{\partial \Phi_{nid}}{\partial z} = \frac{\Phi_{nid}}{2b}\left(1+\frac{R^4}{a^4}-\frac{z^2}{b^2}-\frac{4zR^4}{ba^4}+\frac{3z^2R^4}{b^2a^4}\right), \qquad a \neq 0 \;\&\; b \neq 0.$$

In order to find $\Phi_{nid}(R,z)$ in region (4) of Fig. 4, we start with the values of Φ_{nid} at the point $Q(\mathrm{a},z_s)$ on the side of the diffusion region (Figure 4) and then calculate Φ_{nid} at any point $P(R,z)$ that lies on the same field line in region (4) to the right of Q. Thus, after setting $(R,z) = (a,z_s)$ in expression (13) for Φ that holds in the diffusion region, we obtain

$$\Phi_{nid}(a,z_s) = f(z_s) = -\Phi_{nid0}\left[\frac{1}{3}-\frac{z_s}{b}+\frac{{z_s}^2}{b^2}-\frac{{z_s}^3}{b^3}\right], \qquad b \neq 0. \qquad (14)$$

Since ideal MHD holds in region (4), $\Phi_{nid}(R,z)$ is constant along the field line ($zR^2 = z_s a^2$) joining Q to P, and so the value of Φ_{nid}at P is simply

$$\Phi_{nid}(R,z) = f\left(\frac{zR^2}{a^2}\right) = -\Phi_{nid0}\left[\frac{1}{3} - \frac{zR^2}{ba^2} + \frac{z^2R^4}{a^2b^2} - \frac{z^3R^6}{a^3b^6}\right], a \neq 0 \;\&\; b \neq 0. \quad (15)$$

The solution for $z < 0$ can be obtained in a similar manner by integrating from $z = -b$. We may now make various deductions from the solution. The reconnection rate depends on the form of ή and is given in order of magnitude by

$$\Psi = \int E_{|\ |}\, \mathrm{ds} \sim 2\mathrm{E}_0\mathrm{b}, \quad (16)$$

where E_0 is the electric field at the center of the diffusion region and $2b$ is the dimension of the diffusion region along the magnetic field direction. In our example, $\mathrm{E}_0 = \mathrm{E}_\mathrm{z}(0,0,0) = \frac{\Phi_{nid0}}{2b} = \acute{\eta} j_0$, where $j_0 = \frac{j_0 B_0}{\mu L_0}$ is the value of the current at the origin, and along the spine, Equation (13) implies that

$$\mathrm{E}_\mathrm{z}(0,0,0) = \frac{\Phi_{nid0}}{2b}\left(1 - \frac{z^2}{b^2}\right),$$

and so the reconnection rate becomes, more accurately,

$$\int_{-b}^{b} \mathrm{E}_\mathrm{z}(0,0,0)\, dz = \frac{4}{3} E_0 b = \frac{2}{3}\Phi_{nid0}. \quad (17)$$

The other feature that we can deduce from the electric field components is the perpendicular plasma velocity given by Equation (9). In particular, on the fan plane ($z = 0$) inside D, $E_R = 0$, $E_\varphi = \frac{\Phi_{nid0}}{2b}\left(1 + \frac{R^4}{a^4}\right), \acute{\eta} j_z = \frac{\Phi_{nid0}}{2b}\left(1 - \frac{R^4}{a^4}\right)$, and $B_R = \frac{B_0 R}{L_0}$ so that there is a rotational component given by

$$\mathbf{v}_\varphi = \frac{(\mathrm{E_z} - \acute{\eta}\mathrm{j_z})B_R}{\mathrm{B}^2} = v_0 \frac{R^3}{a^3},$$

where $v_0 = \frac{\Phi_{nid0} L_0}{\left[baB_0\left(1+\frac{1}{4}{j_0}^2\right)\right]}$. The nature of the flow becomes clear if we subtract a component parallel to B in order that v_z=0 (we are free to do this since the component of v parallel to **B** is arbitrary in the model). After doing this we find that v_R vanishes, leaving $v = \left(0, v_\varphi, 0\right)$ i.e., the flow corresponds to a pure rotation (as in the solutions of Ref. 10).

5- GENERLISED MODEL FOR TORSIONAL SPINE RECONNECTION

We now investigate how the properties of the solution vary when the rotational symmetry of the above system is broken. When the rotational symmetry is lost it is no longer possible to find closed-form expressions for the field line mapping. We therefore numerically integrate B to find field lines and solve Equations (6, 8 and 9) on a rectangular grid. We may break the symmetry either in the potential component $\boldsymbol{B}_P$ defining the magnetic null or in the component $\boldsymbol{B}_J$ defining the current tube. Our new potential component of the magnetic field is given by

$$\boldsymbol{B}_P = \left[\frac{2}{k+1}x, \frac{2k}{k+1}y, -2z\right] \qquad (18)$$

in Cartesian coordinates where $k > 0$ is a parameter. As k varies the magnetic field along the spine direction is fixed while the ratio between the fan eigenvalues (associated with the eigenvectors along the $\hat{\boldsymbol{x}}$, $\hat{\boldsymbol{y}}$ and directions) varies. We choose to break the symmetry in $\boldsymbol{B}_J$ by converting to Cartesian coordinates and setting

$$\boldsymbol{B}_J = \begin{cases} j\left[1-\left(\frac{R}{a}\right)^6\right]^4\left[1-\left(\frac{z}{b}\right)^4\right]^2[-qy, x, 0], & R < a,\ z^2 < b^2 \\ [0,0,0] & otherwise \end{cases} \qquad (19)$$

where $R^2 = x^2 + qy^2$ (note that this reduces to expression (10) when $q = 1$). This has the effect of distorting the current into a cylinder with elliptical cross-section, with major and minor axes along the x- and y-axes, extending to$x = \pm a, y = \pm a/\sqrt{q}$. Pre-empting the results of the following section, we present here results for $k = q$, such that as p increases the current tube narrows along the direction associated with the large fan eigenvalue, i.e. the strong field direction in the fan. We set $B_0 = L_0 = \acute{\eta}_0 = j = 1, a = 1, b = 4$, and solve Eqs. (6,8 and 9) on a rectangular grid with 81 gridpoints in each direction covering the volume $-2 < x, y < 2, 0 < z < 4$ with the solution being symmetric about $z = 0$. We restrict our attention to the range$k \geq 1$, which simply selects the $\hat{\boldsymbol{y}}$ direction as the strong field direction in the fan. The results of the above analysis are presented. As k is increased, the current tube shrinks in the y-direction, with the dominant current component $\boldsymbol{J}_z$ intensifying in the part of the tube close to the y-axis (i.e. the direction of the short axis of the ellipse). The stronger current in this region results in an enhanced plasma flow speed. The direction of the flow is also distorted from the circular pattern at $k = 1$, but continues to flow on closed elliptical paths around the spine (z-axis). As the fan plane is approached the radii of the elliptical shells of positive and negative azimuthal flow increase, owing to the hyperbolic nature of the field structure. In order to determine the reconnection rate we calculate “as defined in Equation (16). Due to the breaking of the symmetry it is no longer clear that the maximal value of “should occur along the spine field line, as was found in previous studies (note that the current modulus has maximum value away from the spine for large k). However, it turns out that indeed the maximum occurs along field lines asymptotically close to the spine for all p. Figure 4 displays the peak value of the current density (which we impose) and the reconnection rate as a function of the degree of asymmetry. It is clear that the peak current scales linearly with $(k = q)$ and that correspondingly the reconnection rate scales linearly with k.

5- CONCLUSION

Here we have presented analytical model for torsional magnetic reconnection at 3D null points. The analytical models included for the first time fully localised current layers (focused at the spine) that determine the boundary of the non-ideal region, thus alleviating the requirement in previous models to have an artificially localized (“anomalous”) resistivity. We also for the first time investigated the particular case where the null point is radially symmetric ($k = 1$), i.e. where the fan eigenvalues are equal. Second time we investigated the generic case where the null point is not radially symmetric, i.e. where the fan eigenvalues are not equal ($k \neq 1$). 3D null points have been demonstrated to be present in abundance in the solar corona, and the same is likely to be true in other astrophysical environments. We have shown that the geometry of the current layers within which torsional spine reconnection occur is strongly dependent on the symmetry of the magnetic field defining the null point. Torsional spine reconnection still occurs in a narrow tube around the spine, but with elliptical cross-section when the fan eigenvalues are different. The eccentricity of the ellipse increases as the degree of asymmetry increases, with the short axis of the ellipse being along the strong field direction. Furthermore, the current profile is not azimuthally symmetric around the spine, but is peaked in these strong field regions.

REFERENCES

1-Priest, E.R. and Forbes, T.G., Magnetic reconnection: MHD theory and applications, Cambridge University Press, Cambridge (2000).
2- C. Parnell, J. Smith, T. Neukirch, and E. R. Priest, Phys. Plasmas **3**, 759 (1996).
3- S. Cowley, Cosm. Electrodyn. **3**, 448 (1973).
4-J. Greene, J. Geophys. Res. **93**(A8), 8583, doi:10.1029/JA093iA08p08583 (1988).
5- D. I. Pontin and K. Galsgaard, J. Geophys. Res. **112**, A03103, doi:10.1029/2006JA011848 (2007).
6-G. Hornig and E. R. Priest, Phys. Plasmas **10**, 2712 (2003).
7-D. I. Pontin, G. Hornig, and E. R. Priest, Geophys. Astrophys. Fluid Dyn. **98**, 407 (2004).
8-D. I. Pontin, G. Hornig, and E. R. Priest, Geophys. Astrophys. Fluid Dyn. **99**, 77 (2005).
9-D. I. Pontin, K. Galsgaard, G. Hornig, and E. R. Priest, Phys. Plasmas **12**, 052307 (2005).
10-D. I. Pontin, A. Bhattacharjee, and K. Galsgaard, Phys. Plasmas **14**, 052106 (2007).